Hawking Radiation & Classical Tunneling: A Numerical Study

A thesis submitted in partial fulfillment of the requirement
for the degree of Bachelor of Science in Physics from
The College of William and Mary

by
Dmitriy Zhigunov

Accepted for: _____

_____
Dr. Eugene R. Tracy, Adviser

_____
Dr. Gina Hoatson

_____
Dr. Nahum Zobin

Williamsburg, VA
Spring 2017

Acknowledgements

I would like to thank my adviser, Dr. Eugene Tracy for advising me on my thesis and allowing me to work on this project. Additionally, I would like to the rest of my committee, Dr. Hoatson and Dr. Zobin, for serving on the committee.

Furthermore, it is necessary for me to thank the Sowden Softbrew™ and Kalita Wave™: two coffee makers which made the last few weeks of writing possible.

Abstract

Unruh [1] demonstrated that black holes have an analogy in acoustics. Under this analogy the acoustic event horizon is defined by the set of points in which the local background flow exceeds the local sound speed. In past work [2], we demonstrated that under a white noise source, the acoustic event horizon will radiate at a thermal spectrum via a classical tunneling process. In this work, I summarize the theory presented in [2] and nondimensionalize it in order to reduce the dynamical equations to one parameter, the coupling coefficient η^2. Since η^2 is the sole parameter of the system, we are able to vary it in a numerical study of the dependence of the transmission coefficient on η^2. This numerical work leads to the same functional dependence of the transmission coefficient on η^2 as predicted in [2].

Contents

1. Introduction & Background **1**

1a. The phase space approach to ray tracing 2

1b. Classical tunneling 7

1c. A heuristic argument for Hawking radiation as tunneling 11

2. Full-Wave Studies of the Unruh Model **15**

2a. Self-adjoint formulation of acoustics in non-uniform media 15

2b. Nondimensionalization 18

2c. Normal form 22

3. Numerical Study **24**

3a. The metaplectic transformation 24

3b. Numerical schemes and their stability 26

3c. Computation of the transmission coefficient 28

4. Conclusions **33**

1. Introduction & Background

In 1975 Hawking [3] showed that black holes should emit radiation equivalent to a thermal spectrum with effective temperature

$$T_{\text{eff}} \propto \frac{1}{M}\,, \tag{1}$$

where M is the mass. Hawking's derivation however assumed the existence of quantum fields at arbitrarily large frequencies, as well as an incomplete theory of how quantum fields behave in curved spacetime, causing much scrutiny (see [1, 4, 5]). As an alternative argument, Unruh [1] demonstrated that a classical analogue to Hawking radiation exists within acoustics. In particular, he theorized that an acoustic black hole, defined by the set of points for which the local background flow exceeds the local sound speed, would radiate acoustic radiation. The analogy went beyond the merely conceptual: with the right assumptions, small perturbations within a fluid have a Lorentzian geometry characterized by an "acoustic metric" [6].

Over time, other analog systems were discovered [5, 7], such as in light propagation in rapidly spinning Bose-Einstein condensates or in gravity wave propagation over a a channel of varying width. The arguments leading to these suggested that Hawking radiation was a phenomena arising purely from Lorentzian geometry [6] along with some sort of "event horizon" at which some local speed of the background resonates with the local group velocity. Jacobson [5] later suggested that the Hawking radiation phenomena can be studied via what is referred to in plasma physics literature as mode conversion; however he did not pursue this plasma physics approach.

A treatment of the problem using plasma physics methodologies was provided by Tracy and Zhigunov [2], who applied the ray phase space methodologies of [8] as well as Brizard's theory of linearized MHD [9] to demonstrate that acoustic Hawking radiation is a tunneling phenomena with a weak coupling between the incoming and outgoing modes. This work suggested that in the case of acoustic black holes, the effective temperature is inversely proportional to the length scale of the system, meaning that it serves the acoustic analog the the black hole mass. The work I present here is a recounting of the work in [2] and a numerical study of the predictions of the theory.

In particular, in Chapter 1 I will present the formalisms of ray tracing and classical tunneling, and then demonstrate how they can be *heuristically* used to derive the Hawking result. The assumptions of this heuristic result will be solidified in Chapter 2, where I will rigorously derive a one-dimensional acoustic model for the system, as well as the normal form for the system near the tunneling region. Finally, Chapter 3 will provide a numerical study of the system derived in Chapter 2 in order to directly compute the tunneling coefficient of the system.

1a. The phase space approach to ray tracing

Ray tracing is a form of short-wavelength asymptotics for linear wave equations, also known as WKB methods. A full derivation of the phase space ray tracing approach is provided by [8]. In this section, I will provide a brief summary of the main results and concepts necessary for the ray phase space analysis of acoustic Hawking Radiation.

By tracing the group path through phase space, a ray identifies the behaviour of a plane wave through a system defined by a linear wave equation or equivalently by a dispersion relation. Begin by considering the multicomponent wave equation of the form

$$\sum_{j=1}^{n} \hat{D}_{m,j}(x, -i\partial_x, i\partial_t) \left|\psi_j(x,t)\right\rangle \equiv \hat{D}\psi = 0\,, \tag{2}$$

where $\hat{D} : \mathscr{L}_2 \to \mathscr{L}_2$ is a Hermitian operator, i.e

$$\langle \hat{D}u \,|\, v\rangle = \langle u \,|\, \hat{D}v\rangle \,. \tag{3}$$

for

$$\langle \hat{u} \,|\, v\rangle = \int u^\dagger v \, dx \,. \tag{4}$$

For simplicity, we will assume that there is only one spatial dimension x. A general presentation is given in [8].

The eikonal approximation assumes that solutions to (2) *locally* look like the plane waves, i.e. they have the form

$$\psi(x,t) = \hat{\mathbf{e}}(x;\omega)A(x)e^{i\Theta(x)-i\omega t} \,, \tag{5}$$

where A and Θ are real functions, and $\hat{\mathbf{e}}$ is a complex vector-valued function; and A and $\hat{\mathbf{e}}$ vary on a much longer spatial scale than the phase Θ.

The relevant phase space for plane wave solutions is position-wavenumber (x,k) space. Ray trajectories in this *ray phase space* correspond to eikonal solutions of (2). These trajectories follow from some ray Hamiltonian $\Omega(x,k;\omega)$ which is derived from the wave operator $\hat{D}$ in a manner to be described shortly.

Let us motivate (5) by first considering the case of constant media. In this case, $\hat{D}$ has no explicit dependence on x and t:

$$\sum_{j=1}^{n} \hat{D}_{m,j}(-i\partial_x, i\partial_t)\psi_j(x,t) = 0 \,. \tag{6}$$

Fourier methods then tell us that solutions of (6) are linear combinations of plane waves:

$$\psi(x,t) = \hat{\mathbf{e}}(k;\omega)Ae^{i(kx-\omega t)} \,. \tag{7}$$

Substituting plane wave solutions into into our constant wave-operator brings out the operator-

symbol relations, $-i\partial_x \leftrightarrow k$ and $i\partial_t \leftrightarrow \omega$. Hence, the wave operator $\hat{D}_{m,n}(-i\partial_x, i\partial_t)$ has an associated *dispersion matrix* $\mathsf{D}_{m,n}(k;\omega)$. The wave equation (6) transforms into the matrix problem,

$$\mathsf{D}(k;\omega)\hat{\mathbf{e}} = 0\,. \tag{8}$$

Hence, plane wave solutions of (2) must have values of k and ω which satisfy $\det \mathsf{D} = 0$. The polarization $\hat{\mathbf{e}}$ then must lie in the corresponding null-space of $\mathsf{D}(k;\omega)$, implying that k and ω must be related: i.e. the implicit mapping theorem applied to the dispersion surface $D(k;\omega) \equiv \det \mathsf{D}(k;\omega) = 0$ implies that we may locally write $k = k(\omega)$ or $\omega = \omega(k)$, whuch are called *dispersion relations*.

For example, consider the wave equation

$$\begin{pmatrix} c\partial_x + \partial_t & \partial_x\partial_t \\ -\partial_x\partial_t & c\partial_x - \partial_t \end{pmatrix} \begin{pmatrix} \psi_a \\ \psi_b \end{pmatrix} = 0\,, \tag{9}$$

where c is a constant. After multiplying through by $-i$, the corresponding dispersion matrix is

$$\mathsf{D}(k;\omega) = \begin{pmatrix} ck - \omega & ik\omega \\ -ik\omega & ck + \omega \end{pmatrix}\,, \tag{10}$$

meaning that k and ω must lie on the dispersion surface defined by

$$D(k;\omega) = \det \mathsf{D}(k;\omega) = (c^2 - \omega^2)k^2 - \omega^2 = 0\,. \tag{11}$$

Solving for the dispersion relation $k(\omega)$ we have two roots:

$$k_\pm(\omega) = \pm\frac{\omega}{\sqrt{c^2 - \omega^2}}\,. \tag{12}$$

The polarizations must then satisfy

$$\begin{pmatrix} xk_{\pm}(\omega) - \omega & ik_{\pm}(\omega)\omega \\ -ik_{\pm}(\omega)\omega & ck_{\pm}(\omega) + \omega \end{pmatrix} \hat{\mathbf{e}}_{\pm}(\omega) = 0 \tag{13}$$

which lead to the polarizations

$$\hat{\mathbf{e}}_{\pm}(\omega) = \begin{pmatrix} \omega \pm \omega\sqrt{1 + k_{\pm}^2(\omega)} \\ ik_{\pm}(\omega)\omega \end{pmatrix}. \tag{14}$$

Therefore plane wave solutions of (9) are given by

$$\begin{pmatrix} \psi_a \\ \psi_b \end{pmatrix} = \hat{\mathbf{e}}_{+}(\omega)Ae^{k_{+}x-\omega t} + \hat{\mathbf{e}}_{-}(\omega)Be^{k_{-}x-\omega t}, \tag{15}$$

where A and B will depend on $k_{\pm}, \hat{\mathbf{e}}_{\pm}$ given by (12) and (14), respectively.

Transitioning to nonconstant media (i.e $\hat{D}$ can have explicit x dependencies), the eikonal solutions (5) are no longer exact. Furthermore, the phase $\Theta(x)$ is longer linear in x. These eikonal solutions are only local plane waves, meaning that definitions of wave quantities such as the wavenumber or the dispersion relation only have meaning locally in x. The local wavenumber $k(x; omega)$ is given by the spacial derivative of the phase:

$$k(x) \equiv \frac{\partial\Theta(x)}{\partial x}. \tag{16}$$

In the eikonal limit, we can then note that $-i\partial_x\psi \approx k\psi$, suggesting that the operator-symbol correspondence $-i\partial_x \leftrightarrow k$ still has a local significance. However, the introduction of a spatial dependence leads to the following issue: in the case of uniform media, the wave operator $\hat{D}$ was composed out of powers of ∂_x and ∂_t, which commute – however, introducing spatial dependence leads to noncommuting objects such as $\hat{x}$ and $-i\partial_x$. This issue is resolved by a formalism known as the Weyl symbol calculus. The Wey symbol calculus provides a linear

map between operators and symbols which preserves the operator algebras. In particular, the associated Weyl symbol $a(x,k)$ of the operator $\hat{\mathscr{A}}$ is given by

$$a(x,k) = \int \left\langle x + \frac{s}{2} \right| \hat{\mathscr{A}} \left| x - \frac{s}{2} \right\rangle e^{-iks}\, ds\,. \tag{17}$$

In general, if $\hat{\mathscr{A}} \leftrightarrow a(x,k)$ and $\hat{\mathscr{B}} \leftrightarrow b(x,k)$ then the associated symbol of the product $\hat{\mathscr{A}}\hat{\mathscr{B}}$ is not equal to the symbol of $\hat{\mathscr{B}}\hat{\mathscr{A}}$. Instead, the associated symbol of the products is given by the *Moyal product* $*$

$$\hat{\mathscr{A}}\hat{\mathscr{B}} \leftrightarrow a(x,k) * b(x,k)\,, \tag{18}$$

where

$$u * v = \sum_{n=0}^{\infty} \left[\left(\frac{i}{2}\right)^n \; u \left(\overleftarrow{\partial_x}\overrightarrow{\partial_k} - \overleftarrow{\partial_k}\overrightarrow{\partial_x} \right)^n v \right]\,. \tag{19}$$

In particular, an important result which we will use is the Weyl correspondence

$$\hat{x}\hat{k} + \hat{k}\hat{x} \leftrightarrow 2xk\,, \tag{20}$$

as well as $x * k = xk + i/2$ and $k * x = xk - i/2$.

The dynamics of eikonal solutions are encoded in the $n \times n$ dispersion matrix $\mathsf{D}(x,k;\omega)$, given by the associated Weyl symbol to the the wave operator $\hat{D}$. In [8] it is shown that for self-adjoint operators $\hat{D}$ the dispersion matrix is Hermitian for all real x, k, and ω. The polarization vectors $\hat{\mathbf{e}}(x,k;\omega)$ are defined as the eigenvectors of $\mathsf{D}(x,k;\omega)$ at each point. Since D is Hermitian, away from degeneracies the eigenvectors are orthogonal. Eikonal solutions to (2) will remain along a given smoothly-varying polarization as long as the eikonal approximation remains valid. The dispersion relation is given by $\Omega(x,k;\omega) \equiv \det \mathsf{D} = 0$, and it serves as the ray Hamiltonian. The trajectories in ray phase space are then governed by[1]

$$\frac{dx}{d\sigma} = \frac{\partial \Omega}{\partial k}\,, \quad \frac{dk}{d\sigma} = -\frac{\partial \Omega}{\partial x}\,, \tag{21}$$

[1]See [8] for a derivation of these facts.

where σ is some arbitrary ray parameter. A set of solutions in terms of the time t may be obtained instead by first solving for the trajectories $t(\sigma)$ and $\omega(\sigma)$ and then reparametrizing. Ultimately, the resulting equations are

$$\frac{dx}{dt} = -\left(\frac{\partial\Omega}{\partial\omega}\right)^{-1}\frac{\partial\Omega}{\partial k}\,, \quad \frac{dk}{dt} = \left(\frac{\partial\Omega}{\partial\omega}\right)^{-1}\frac{\partial\Omega}{\partial x}\,, \tag{22}$$

where the term $-\left(\frac{\partial\Omega}{\partial\omega}\right)^{-1}\frac{\partial\Omega}{\partial k}$ is the group velocity v_g. For time-stationary systems, the amplitude A follows the rule of action conservation,

$$\frac{\partial}{\partial x}\left(\mathscr{J}\, v_g\right) = 0\,, \tag{23}$$

where the action $\mathscr{J} \propto A^2$. Therefore.

$$A^2 v_g = constant\,. \tag{24}$$

All together, we may then reconstruct the eikonal solution from the ray trajectories

$$\psi(x,t) = \hat{\mathbf{e}}(x,t)A(x,t)e^{\int_{x_0}^{x} k\,dx - \omega t}\,. \tag{25}$$

1b. Classical tunneling

Tunneling through steep potential barriers is usually discussed in introductory quantum mechanics courses. However, tunneling is a very general phenomenon that occurs in many different areas of science and engineering, where it masquerades itself through a variety of names such as "avoided crossings," "Landau-Zener crossings," "resonance crossing," etc. It may occur in any oscillatory system with slowly varying parameters – hence it is encountered in plasma physics as well. The goal of this section is to attempt to generalize the concept of

scalar tunneling. Let us begin by considering the the nondimensional Schrödinger equation,

$$\left(-\frac{d^2}{dx^2} - \alpha x^2 + \omega\right)\psi = 0\,. \tag{26}$$

This is equivalent to an inverted harmonic oscillator potential given by $V = -\alpha x^2$. The corresponding dispersion surface is given by

$$D(x, k; \omega) = k^2 - \alpha x^2 + \omega = 0\,. \tag{27}$$

A plot of this surface is given in Figure 1. Far from the origin, the eikonal approximation remains valid. However, between $x = \pm\sqrt{\omega/\alpha}$, there exist no real solutions for k. This "evanescent" region corresponds to the region where tunneling occurs. From a ray tracing perspective, this can be understood as a coupling between disjoint regions of the dispersion surface $D(x, k; \omega)$.

The eikonal approximation is not valid within the evanscent region, nor in the vicinity of the turning points. However, it is possible to "connect" eikonal solutions to the exact solutions in the tunneling region. In more general problems, the form (27) is only locally valid near the tunneling region, so the matching to eikonal solutions outside the tunneling region becomes a method for constructing approximate solutions everywhere.

Hamilton's ray equations (22) for the dispersion function (27) are

$$\frac{dx}{dt} = -2k\,, \quad \frac{dk}{dt} = 2\alpha x\,. \tag{28}$$

The group velocity $v_g \equiv dx/dt$ is given by $-2k$, hence the amplitude is given by

$$A \propto \frac{1}{\sqrt{2k}} = \frac{1}{\left(4(\alpha x^2 - \omega)\right)^{1/4}}\,. \tag{29}$$

The direction of energy flow on the rays is indicated in Figure 1. This is important for proper

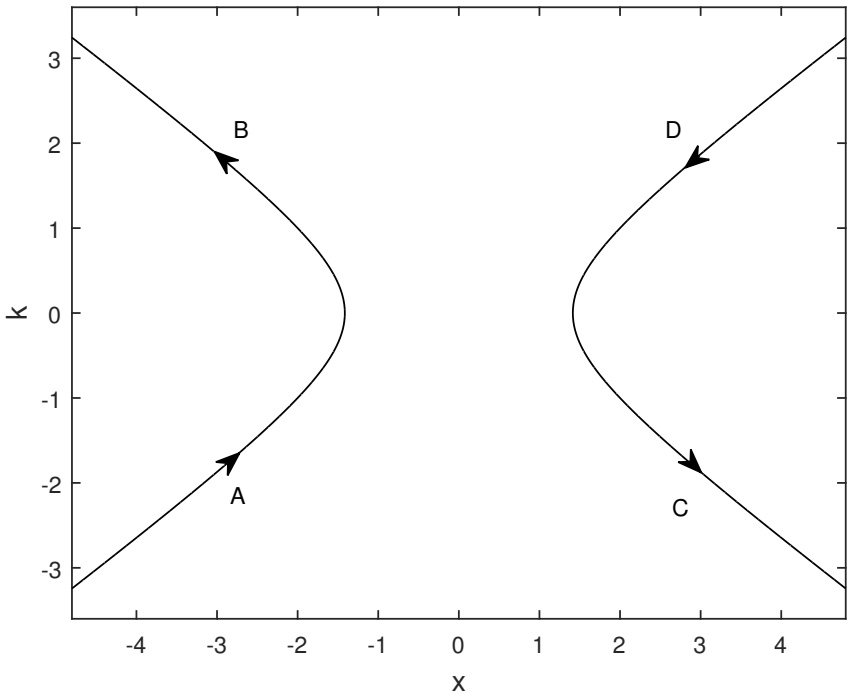

Figure 1. The surface $D(x, k; \omega) = 0$ given by (27) plotted with $\alpha = 1/2$ and $\omega = 1$. The arrows represent the direction of the group velocity along the surface.

assignment of boundary conditions, which we will discuss in detail in Chapter 3. Away from the tunneling region, the full eikonal solutions may then be constructed as in the previous section.

The general solutions of (26) are known as the parabolic cylinder functions [10]. The transmission between modes is given by

$$\tau \equiv e^{-\pi\eta^2}\,, \tag{30}$$

where

$$\eta \equiv \frac{1}{2}\sqrt{\frac{\omega}{\alpha}}\,, \tag{31}$$

is the coupling coefficient. This means that a ray with action $\mathscr{J}$ incoming on ray A is transmitted to ray C with action $\tau^2\,\mathscr{J}$ and reflected along ray D with action $(1-\tau^2)\,\mathscr{J}$, and likewise for modes coming in through ray B.

As long as a as the dispersion relation of a system Taylor expands into the form (27) near the tunneling region, the solutions near the tunneling region behave like parabolic cylinder functions. Outside of the tunneling region, the eikonal approximation holds, and we can match to ray solutions. We also need two results, both of which are discussed in greater detail in [8]:

1. Linear canonical transformations in ray phase space correspond to metaplectic transformations on the original wave equation. This allows us to change representation in order to put the system into the simplest possible form, and to deal with challenges in the numerical solution to the Hawking problem (see Chapter 3).

2. Metaplectic transformations preserve tunneling coefficients. This is because they are unitary transformations; hence energy is conserved.

Regardless of the representation, the physics of a given system remains unchanged – hence the tunneling coefficient is preserved. Therefore, (27) serves as a local normal form for not only systems resembling (26), but also for any system whose dispersion relation can be transformed into (27) by a linear canonical transformation of the form

$$\begin{pmatrix} x' \\ k' \end{pmatrix} = \mathsf{M} \begin{pmatrix} x \\ k \end{pmatrix} , \tag{32}$$

where M is a symplectic matrix:

$$\mathsf{M}^\dagger \mathsf{J} \mathsf{M} = \mathsf{J} , \tag{33}$$

for the symplectic matrix

$$\mathsf{J} = \begin{pmatrix} 0 & 1 \\ -1 & 0 \end{pmatrix} . \tag{34}$$

This will be fundemental in the construction of the numerical schemes in Chapter 3.

1c. A heuristic argument for Hawking radiation as tunneling

The case for the existence of a Hawking radiation analogue in acoustics was sufficiently made in [1], and a rigorous derivation of the acoustic metric is provided in [7]. Most analyses of these arguments (for instance [1, 5–7]) discussed acoustic black holes exclusively in terms of their significance to actual black holes. However, it remains of interest that acoustic Hawking radiation is a general linear wave phenomenon. As such, the work presented here attempts to distance ourselves from the black hole analogy and instead isolate the classical physics.

We begin by recalling the acoustic wave equation:

$$c_s^2 \frac{\partial^2 \psi}{\partial x^2} - \frac{\partial^2 \psi}{\partial t^2} = 0\,. \tag{35}$$

Here c_s is assumed to be constant. The dispersion relation is

$$D(k;\omega) = \omega^2 - c_s^2 k^2 = (\omega + c_s k)(\omega - c_s k) = 0\,. \tag{36}$$

Therefore, $\omega = \pm c_s k$. The group velocity in is given by

$$v_g(k) = -\left(\frac{\partial D}{\partial \omega}\right)^{-1} \frac{\partial D}{\partial k} = \frac{c_s^2 k}{\omega} = \pm c_s\,, \tag{37}$$

meaning that the group velocity is $+c_s$ for positive k and $-c_s$ for negative k.

Introducing a constant, background flow v, the Doppler effect means we take $\omega \to \omega - vk$. Therefore,

$$D(k;\omega) = \left(\omega - (v + c_s)k\right)\left(\omega - (v - c_s)k\right)\,. \tag{38}$$

The wave propagating upstream (against the flow) and downstream (with the flow) have group velocities $v_g = v - c_s$ and $v_g = v + c_s$, respectively.

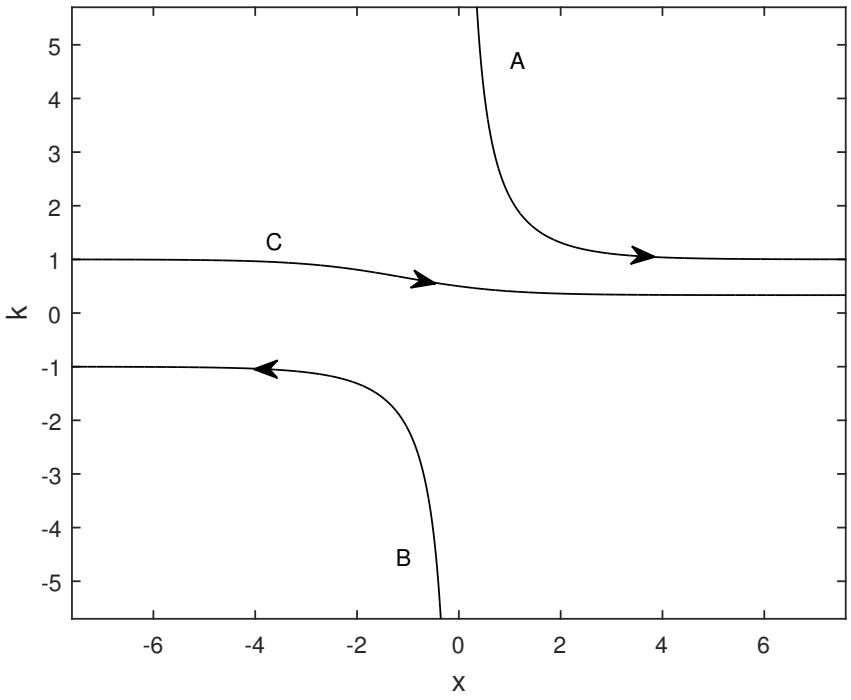

Figure 2. The surface $D(x, k; \omega) = 0$ given by (39) with $v(x) = c_s(1 + \tanh(x/2))$, $c_s = 1$, and $\omega = 1$. The arrows represent the direction of energy flow along the ray.

Now consider a spatially dependent flow, $v(x)$. On physics grounds, if the flow varies smoothly and the length scale of the variation is long compared to k^{-1}, we might expect the local dispersion relation to be

$$D(x, k; \omega) = (\omega - (v(x) + c_s)k)\,(\omega - (v(x) - c_s)k)\ . \tag{39}$$

A rigorous derivation of the corresponding wave equation for one dimensional acoustic is given in the next section.

The point when $v(x) = c_s$ corresponds to the acoustic "event horizon." An example of such a dispersion relation is given in Figure 2. In this case, the acoustic event horizon occurs at $x = 0$, to the right of which which there are no left-moving modes. We can note that ignoring the "incoming mode," C, this dispersion relation appears to be a rotated version of the one presented in Figure 1.

To make this correspondence concrete, we begin by linearizing the background flow near the event horizon as $v \approx c_s(1+x/L)$ for some length scale L. The dispersion relation is then given by

$$D(x,k;\omega) = \left(\omega - \left(2+\frac{x}{L}\right)ck\right)\left(\omega - \frac{c_s x k}{L}\right) \equiv D_1(x,k;\omega)D_2(x,k;\omega)\,. \tag{40}$$

Focusing on the tunneling branch D_2, the dispersion relation simply becomes

$$D_2(x,k;\omega) = \omega - \frac{c_s x k}{L} = \frac{c_2}{L}\left(\eta^2 - xk\right)\,. \tag{41}$$

Through the Weyl correspondence, we obtain the local wave equation

$$\left[\frac{i}{2}\left(x\frac{\partial}{\partial x} + \frac{\partial}{\partial x}x\right) + \eta^2(\omega)\right]\phi(x) = 0\,, \tag{42}$$

for $\eta^2 = \omega L/c_s$. The solution is

$$\phi(x) = \begin{cases} a_+ x^{i\eta^2 - 1/2}\,, & x > 0 \\ a_- |x|^{i\eta^2 - 1/2}\,, & x < 0 \end{cases}\,. \tag{43}$$

A rather technical calculation of the transmission and conversion coefficients is given in [2]. The result is given by

$$\tau = e^{-\pi\eta^2} = e^{-\pi\omega L/c_s}\,. \tag{44}$$

An analogy to Hawking radiation can be made as follows. Consider some white noise source infinitesimally close to the event horizon on A. The exponent in (44) is linear in ω; hence it looks like a Boltzmann factor

$$e^{-\hbar\omega/k_b T_{\text{eff}}}\,, \tag{45}$$

with

$$T_{\text{eff}} = \frac{\hbar c_s}{\pi k_b L} \,. \tag{46}$$

In this case, the effective temperature of the acoustic event horizon is inversely proportional to the length scale L. Therefore, it appears that in acoustic analogy, the length scale serves as a substitute for the black hole mass.

Due to the essential singularity of the solutions (43) at $x = 0$, numerical integration of the system is difficult. Instead, if we wish to numerically calculate the transmission coefficient, we must change representation. We can then define a new canonical pair (X, K) given by

$$x = \frac{1}{\sqrt{2}} (X - K) \,, \quad k = \frac{1}{\sqrt{2}} (X + K) \,. \tag{47}$$

In terms of these coordinates, the dispersion relation is given by

$$D_2(X, K; \omega) = \omega - \frac{c_s}{2L}(X^2 - K^2) \,. \tag{48}$$

Note that this is the exact form of (27). There are no essential singularities in the parabolic cylinder functions, leading to straightforward numerical integration.

2. Full-Wave Studies of the Unruh Model

In this section I will summarize the major results of the theory, as well as lay down the groundwork necessary for the numerical study of our system .

2a. Self-adjoint formulation of acoustics in non-uniform media

Here I will outline the derivation presented by Tracy and Zhigunov [2] for a variational formulation of one-dimensional acoustics in non-uniform media. As mentioned in Chapter 1, such a formulation suggests that acoustic Hawking radiation may be described as a classical tunneling problem. In particular, the variational formulation allows for the application of the ray tracing formalism presented in [8], which is suggestive that acoustic Hawking radiation can be described as classical tunneling.

Following the formalism in [9], let us introduce a one-dimensional ideal fluid with density $\rho(x,t)$, pressure $p(x,t)$, and velocity $v(x,t)$. Assuming adiabatic behaviour, these quantities obey the evolution equations:

$$\frac{\partial \rho}{\partial t} + \frac{\partial \rho v}{\partial x} = 0\,, \tag{49}$$

$$\rho\left(\frac{\partial v}{\partial t} + v\frac{\partial v}{\partial x}\right) + \frac{\partial p}{\partial x} = 0\,, \tag{50}$$

$$\frac{\partial p}{\partial t} + v\frac{\partial p}{\partial x} + \gamma p\frac{\partial v}{\partial x} = 0\,, \tag{51}$$

where γ is the ratio of specific heats. Now consider time-stationary but spatially nonuniform backgrounds with flow $p_0(x), \rho_0(x), v_0(x)$. Acoustic waves correspond to small perturbations of $\rho(x,t)$, $p(x,t)$, and $v(x,t)$ with respect to this background. We linearize the field variables of (49-51) as $p(x,t) = p_0(x)+\epsilon p_1(x,t)$, $\rho(x,t) = \rho_0(x)+\epsilon\rho_1(x,t)$ and $v(x,t) = v_0(x)+\epsilon v_1(x,t)$, for some formal small parameter ϵ. Substituting back into (49-51) leads to the zeroth order evolution equations:

$$\frac{\partial \rho_0 v_0}{\partial x} = 0\,, \tag{52}$$

$$\frac{\partial}{\partial x}\left(\frac{1}{2}\rho_0 v_0^2 + p_0\right) = 0\,, \tag{53}$$

$$v_0\frac{\partial p_0}{\partial x} + \gamma p_0\frac{\partial v_0}{\partial x} = 0\,, \tag{54}$$

and the evolution equations for the first order evolution:

$$\frac{\partial \rho_1}{\partial t} + \frac{\partial}{\partial x}\left(\rho_0 v_1 + \rho_1 v_0\right) = 0\,, \tag{55}$$

$$\rho_0\frac{\partial v_1}{\partial t} + \frac{1}{2}\rho_1\frac{\partial}{\partial x}\left(v_0^2\right) + \rho_0\frac{\partial v_0 v_1}{\partial x} + \frac{\partial p_1}{\partial x} = 0\,, \tag{56}$$

$$\frac{\partial p_1}{\partial t} + \left(v_0\frac{\partial p_1}{\partial x} + \gamma p_1\frac{\partial v_0}{\partial x}\right) + \left(v_1\frac{\partial p_0}{\partial x} + \gamma p_0\frac{\partial v_1}{\partial x}\right) = 0\,. \tag{57}$$

Following [9] we replace the first order fields with the particle displacement field ξ given by the identities

$$\rho_1 + \frac{\partial \rho_0\xi}{\partial x} = 0\,, \tag{58}$$

$$v_1 + \xi\frac{\partial p_0}{\partial x} - v_0\frac{\partial \xi}{\partial x} + \xi\frac{\partial v_0}{\partial x} = 0\,, \tag{59}$$

$$p_1 + \xi\frac{\partial p_0}{\partial x} + \gamma p_0\frac{\partial \xi}{\partial x} = 0\,. \tag{60}$$

This quantity measures the displacement of a fluid particle around some point x. Substitution of these identities into the first order evolution equations (55-57) leads to the evolution

equation for the particle displacement:

$$\rho_0 \frac{\partial^2 \xi}{\partial t^2} + 2\rho_0 v_0 \frac{\partial^2 \xi}{\partial x \partial t} = \frac{\partial}{\partial x}\left((\gamma p_0 - \rho_0 v_0^2) \frac{\partial \xi}{\partial x} \right) . \tag{61}$$

In the simplest case where ρ_0 and p_0 are constant, and $v_0 = 0$, after some rearranging this equation reduces to the standard wave equation:

$$\frac{\partial^2 \xi}{\partial t^2} - c_s^2 \frac{\partial^2 \xi}{\partial x^2} = 0 \,, \tag{62}$$

where $c_s^2 = \gamma p_0 / \rho_0$ is the sound speed.

Returning to the general form with nonconstant backgrounds, it is possible to demonstrate that (61) follows from the variational principle

$$\mathscr{A}[\xi] = \frac{1}{2} \iint \left[\rho_0 \left(\frac{\partial \xi}{\partial t} + v_0 \frac{\partial \xi}{\partial x} \right)^2 - \gamma p_0 \left(\frac{\partial \xi}{\partial x} \right)^2 \right] dx \, dt \,, \tag{63}$$

where the factor of $1/2$ was introduced so that the canonical momentum density matches the physics momentum density. In order to perform a ray phase space analysis of this system, we will find it useful to introduce a Hamiltonian formulation. We start by introducing the canonical momentum density conjugate to ξ:

$$\pi \equiv \frac{\delta \mathscr{A}}{\delta \xi_t} = \rho_0 \left(\frac{\partial \xi}{\partial t} + v_0 \frac{\partial \xi}{\partial x} \right) , \tag{64}$$

where $\xi_t \equiv \partial_t \xi$. The Hamiltonian density is given through the Legendre transformation

$$\begin{aligned} \mathscr{H} &\equiv \pi \xi_t - \mathscr{A} \\ &= \iint \left(\frac{\pi^2}{2\rho_0} - \pi v_0 \frac{\partial \xi}{\partial x} - \frac{p_0 \xi}{2} \frac{\partial^2 \xi}{\partial x^2} \right) dx \, dt \,. \end{aligned} \tag{65}$$

Hamilton's equations for the system are

$$\frac{\partial \xi}{\partial t} = \frac{\delta \mathscr{H}}{\delta \pi}\,, \quad \frac{\partial \pi}{\partial t} = -\frac{\delta \mathscr{H}}{\delta \xi}\,, \tag{66}$$

Leading to the evolution equation

$$\frac{\partial}{\partial t}\begin{pmatrix} \xi \\ \pi \end{pmatrix} = \begin{pmatrix} -v_0\partial_x & \rho_0^{-1} \\ \rho_0 c_s^2 \partial_x^2 & -\partial_x v_0 \end{pmatrix}\begin{pmatrix} \xi \\ \pi \end{pmatrix}\,, \tag{67}$$

where I have divided through by an overall factor of i.

2b. Nondimensionalization

In the numerical study in the following chapter, we will examine the behaviour of the system as we vary the parameters. It is thus crucial the we nondimenionalize in order to identify the most important parameters. Let us define $\psi_a = \xi$, $\rho_*\omega_0\psi_b = \pi$, $t = T\tau$, and $x = L\chi$. Performing the proper substitutions, the system becomes

$$\frac{\partial}{\partial \tau}\begin{pmatrix} \psi_a \\ \psi_b \end{pmatrix} = T\begin{pmatrix} -L^{-1}v_0\partial_{\chi'} & \omega_0\rho_*\rho_0^{-1} \\ \omega_0^{-1}\rho_*^{-1}\rho_0 L^{-2}c_s^2\partial_\chi^2 & -L^{-1}\partial_\chi v_0 \end{pmatrix}\begin{pmatrix} \psi_a \\ \psi_b \end{pmatrix}\,. \tag{68}$$

Evidently, the proper choices are $\omega_0 = T^{-1}$, $L = Tc_s$, and $\rho_* = \rho_0$. Additionally, we can nondimensionalize v_0 by defining $v_0 = c_s g(\chi)$ which makes our equations

$$\frac{\partial}{\partial \tau}\begin{pmatrix} \psi_a \\ \psi_b \end{pmatrix} = \begin{pmatrix} -g\partial_\chi & 1 \\ \partial_\chi^2 & -\partial_\chi g \end{pmatrix}\begin{pmatrix} \psi_a \\ \psi_b \end{pmatrix}\,. \tag{69}$$

Equivalently:

$$\begin{pmatrix} \partial_\tau + g\partial_\chi & -1 \\ -\partial_\chi^2 & \partial_\tau + \partial_\chi g \end{pmatrix}\begin{pmatrix} \psi_a \\ \psi_b \end{pmatrix} = 0\,. \tag{70}$$

Note that this operator is not self-adjoint with respect to the standard inner product. However, following from Brizard's work on linearized MHD [9], we know that this operator is self-adjoint with respect to a symplectic inner product. Hence, we can multiply the symplectic matrix

$$\mathsf{J} \equiv \begin{pmatrix} 0 & 1 \\ -1 & 0 \end{pmatrix}, \tag{71}$$

in order to arrive at the equivalent expression:

$$\begin{pmatrix} -\partial_\chi^2 & \partial_\tau + \partial_\chi g \\ \partial_\tau - g\partial_\chi & -1 \end{pmatrix} \begin{pmatrix} \psi_a \\ \psi_b \end{pmatrix} \equiv \hat{D}\Psi = 0\,. \tag{72}$$

The operator $\hat{D}$ is self-adjoint under the standard inner product,

$$\langle u \,|\, v \rangle = \int u^\dagger v \, dx\,, \tag{73}$$

meaning we may apply the formalism of Section 1a.

Recall that Weyl symbol calculus gives us

$$i\partial_\tau \leftrightarrow \omega, \quad -i\partial_\chi \leftrightarrow k\,. \tag{74}$$

Therefore, the symbol associated with $\hat{D}$ of (72) is

$$\mathsf{D}(\chi, k) = \begin{pmatrix} k^2 & -i\omega + ik * g \\ i\omega - ig * k & 1 \end{pmatrix} \tag{75}$$

where $*$ denotes the Moyal product. Eventually, we will linearize the background as $g = 1 + \alpha\chi$, though for notational convenience, we will keep using g. Thus $g * k = gk + \frac{\alpha i}{2}$ and

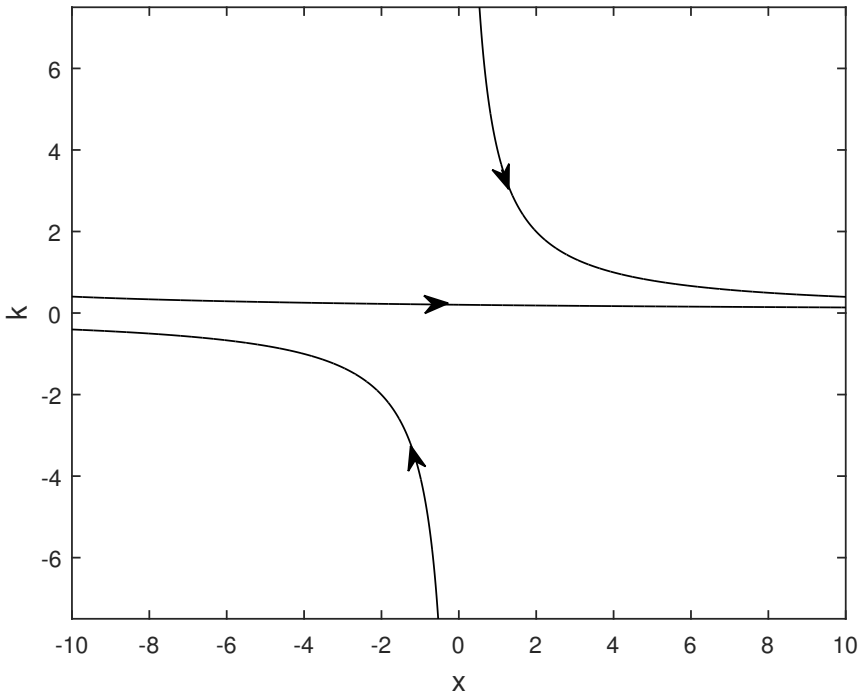

Figure 3. The dispersion surface $\det \mathsf{D}(\chi, k) = 0$ with $\omega = 0.4$ and $\alpha = 0.1$.

$k * g = gk - \frac{\alpha i}{2}$. So it is convenient to write

$$\mathsf{D}(\chi, k) = \begin{pmatrix} k^2 & -i\omega + igk + \frac{\alpha}{2} \\ i\omega - igk + \frac{\alpha}{2} & 1 \end{pmatrix} . \tag{76}$$

The corresponding dispersion relation to (76) is seen in Figure 3. Not shown, is the false horizon corresponding to when $g = -1$.

Though the form of (76) has isolated a large portion of the dynamics, it is possible to go further. We begin by noting that congruence transformations on the dispersion matrix D preserves the null space of D. Hence, the solutions of the corresponding system $\hat{D}\Psi = 0$ remain invariant under congruence.

I begin by defining the rescaled phase space variables $\chi' = \alpha^{-1}\chi$ and $k' = k\alpha$. The rescaled background flow is then given by $g'(\chi') = 1 + \alpha\chi'$. In terms of the rescaled variable, the

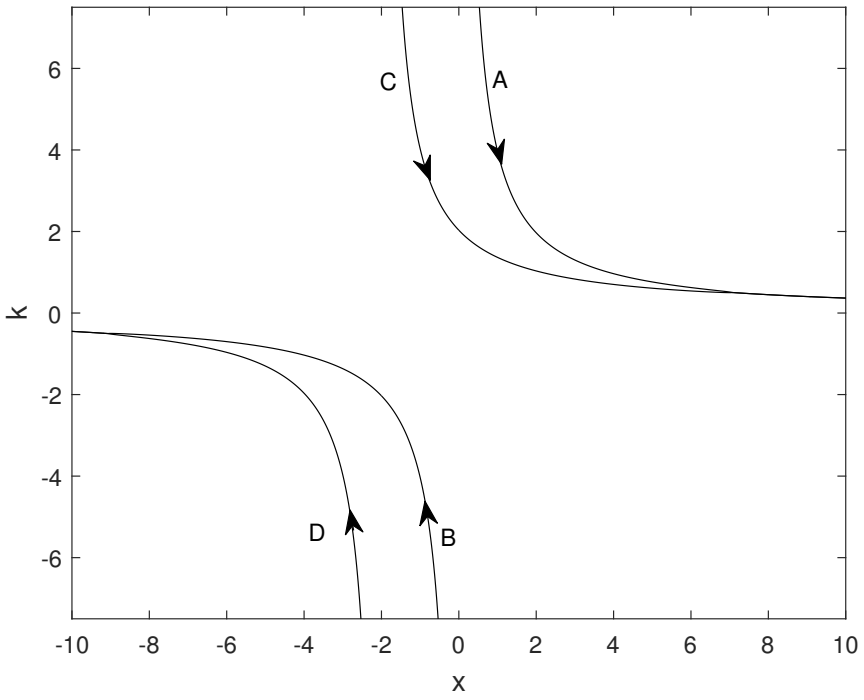

Figure 4. The dispersion surface $\det \mathsf{D}'(\chi', k) = 0$ with $\eta^2 = 4$.

dispersion matrix is given by

$$\mathsf{D}(\chi', k') = \begin{pmatrix} \alpha^2 k'^2 & -i\omega + i\alpha k' + i\alpha\chi' k' + \frac{\alpha}{2} \\ i\omega - i\alpha k' - i\alpha\chi' k' + \frac{\alpha}{2} & 1 \end{pmatrix} . \tag{77}$$

Recalling that the definition $\eta^2 = \omega/\alpha$, we perform a congruence transformation using the matrix

$$\mathsf{Q} = \begin{pmatrix} \alpha^{-1} & 0 \\ 0 & 1 \end{pmatrix} , \tag{78}$$

to define the new dispersion matrix

$$\mathsf{D}'(\chi', k') \equiv \mathsf{Q}\mathsf{D}\mathsf{Q}^\dagger = \begin{pmatrix} k'^2 & i(k' + k'\chi' - i/2) - i\eta^2 \\ -i(k + \chi' k' + i/2) + i\eta^2 & 1 \end{pmatrix} . \tag{79}$$

The resulting dispersion curves given by (79) are seen in Figure 4. The linearization of

the background $g'(\chi', k')$ introduces a "false" event horizon at $\chi' = -2$. However, this event horizon lies on a different polarization than the one of interest. In particular, modes A and B lie on one polarization whereas modes C and D lie on the other. As we will see in the following section, the coupling between these polarizations is small. Hence, they appear as two separate tunneling processes.

2c. Normal form

In this case, when considering systems with the same normal form, we are looking for systems related to each other by congruence. For simplicity, we will disregard the Moyal terms. They can be included in higher order studies, but that significantly complicates the algebra without contributing much additional insight. For a thorough discussion of higher order effects see [11]. Thus the dispersion matrix we are considering is given by

$$\mathsf{D}(\chi, k) = \begin{pmatrix} k^2 & i(k + k\chi - \eta^2) \\ -i(k + k\chi - \eta^2) & 1 \end{pmatrix}. \tag{80}$$

We have found that to best isolate the behavior of the system we shift k so that it is centered around the value of the incoming mode at the resonance $k_0 = \eta^2/2$ – i.e. $k = k_0 + \kappa$.

Using the dispersion matrix defined in (80), I wish to return to the approach of [2]. The relevant polarization is not the eigenvectors of D but of JD. Ignoring the Moyal terms, these polarizations are given by

$$\hat{\mathbf{e}}_\pm = \frac{1}{\sqrt{2k_0}} \begin{pmatrix} 1 \\ \\ \mp i k_0 \end{pmatrix}. \tag{81}$$

These eigenvectors are not orthogonal with respect to the Cartesian inner product, but they

are with respect to the symplectic inner product. We define the matrix Q as

$$\mathsf{Q} = [\hat{\mathbf{e}}_+ \, , \, \hat{\mathbf{e}}_-] = \frac{1}{\sqrt{2k_0}} \begin{pmatrix} 1 & 1 \\ -ik_0 & ik_0 \end{pmatrix} . \tag{82}$$

Performing a congruence transformation on D using Q, we have

$$\mathsf{Q}^\dagger \mathsf{D} \mathsf{Q} \approx \begin{pmatrix} (x+2)(k_0+\kappa) - \eta^2 & \kappa \\ \kappa & -x(k_0+\kappa) + \eta^2 \end{pmatrix} . \tag{83}$$

where we have expanded to first order in κ.

The normal form (83) suggests that at the resonance ($x = 0$, $\kappa = 0$), the incoming and outgoing modes lie primarily on the diagonals of (83), with a coupling of κ, which is small. Therefore, we expect that the assumptions of scalar tunneling discussed in Chapter 1 to be valid.

3. Numerical Study

Up until now, all the work presented has been to set up the system so as to make analytical predictions. Derivation of the Hawking result in Chapter 1 requires certain simplifying assumptions, to which the normal form is only suggestive. Therefore, the issues discussed in this chapter concern strictly numerical aspects of our system, where we perform a direct simulation of the transition region and numerically extract the transmission coefficient.

3a. The metaplectic transformation

For the numerical work, we return to (79). The rays follow the contours of the surface $\det \mathsf{D}'(\chi, k) = 0$, seen in Figure 4. However, this suggests that near the event horizon we will have arbitrarily high wavenumbers. This is reflected in the local solution derived in Section 1c, where we showed that in the x representation, the tunneling wave function has an essential singularity (see(43)). Numerically, this means that for any choice of grid size, we will encounter wavelengths which we cannot resolve. Thus it is unclear whether a numerical scheme will be able to resolve the tunneling phenomena in the x representation.

To avoid this issue we perform a 45° rotation in phase space by defining the canonical pair X, K to satisfy

$$\chi' = \frac{1}{\sqrt{2}}\,(X - K)\ , \quad k' = \frac{1}{\sqrt{2}}\,(X + K)\ . \tag{84}$$

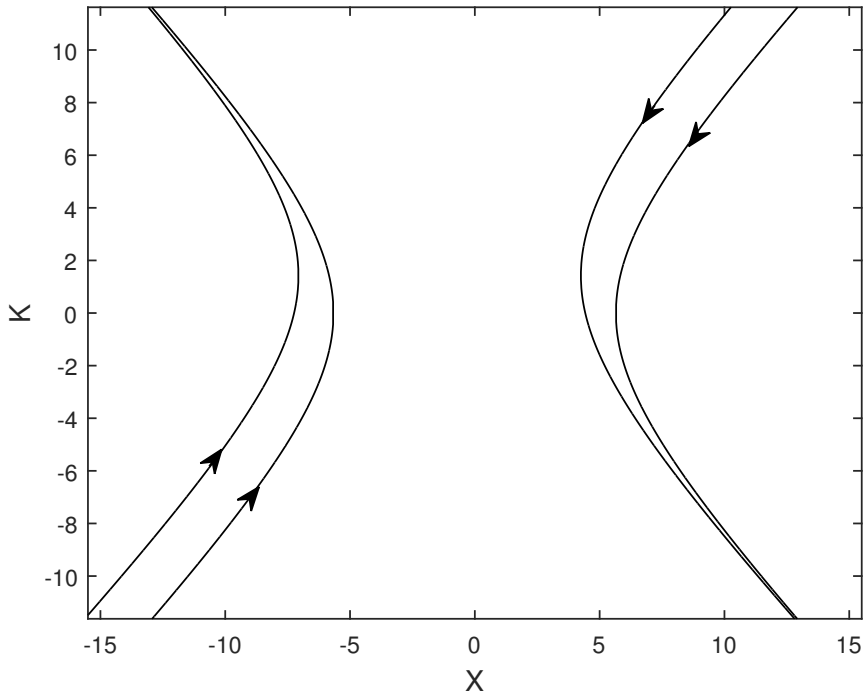

Figure 5. The surface $\det \mathsf{D}'(X,K) = 0$ for $\eta^2 = 4$.

The new dispersion surface is seen in Figure 5 and new dispersion matrix is given by,

$$\mathsf{D}'(X,K) = \begin{pmatrix} \frac{1}{2}\left(X^2 + 2XK + K^2\right) & i\left(\frac{1}{\sqrt{2}}X + \frac{1}{\sqrt{2}}K + \frac{1}{2}X^2 - \frac{1}{2}K^2 - \eta^2 - \frac{i}{2}\right) \\ -i\left(\frac{1}{\sqrt{2}}X + \frac{1}{\sqrt{2}}K + \frac{1}{2}X^2 - \frac{1}{2}K^2 - \eta^2 + \frac{i}{2}\right) & 1 \end{pmatrix}. \tag{85}$$

Note: there are no additional Moyal terms in the off-diagonal entries since they have been previously calculated in (79). Additionally, I have used the fact that $X * K + K * X = 2XK$.

The Weyl symbol calculus allows us to associate the operators

$$X \leftrightarrow \hat{X}\,, \quad K \leftrightarrow -i\partial_X\,. \tag{86}$$

Hence, the associated wave equation of $D(X,K)$ is then given by

$$\begin{aligned}\left(\frac{1}{2}X^2-\frac{i}{2}X\partial_X-\frac{i}{2}\partial_X X-\frac{1}{2}\partial_X^2\right)\Psi_a\\ +\left(\frac{1}{\sqrt{2}}\partial_X+\frac{i}{\sqrt{2}}X+\frac{i}{2}\partial_X^2+\frac{i}{2}X^2-i\eta^2+\frac{1}{2}\right)\Psi_b=0\,,\end{aligned}\tag{87}$$

$$\left(\frac{1}{\sqrt{2}}\partial_X-\frac{i}{\sqrt{2}}X-\frac{i}{2}\partial_X^2-\frac{i}{2}X^2+i\eta^2+\frac{1}{2}\right)\Psi_a+\Psi_b=0\,.\tag{88}$$

3b. Numerical schemes and their stability

The differential equations, (87) and (88) can be discretized directly and then integrated numerically. We will use the scheme

$$\begin{aligned}\partial_X\Psi&\to\frac{\Psi_{j+1}-\Psi_{j-1}}{2h}\,, & \partial_X^2\Psi&\to\frac{\Psi_{j+2}-2\Psi_j+\Psi_{j-2}}{4h^2}\,,\\ X\partial_X\Psi&\to X_j\frac{\Psi_{j+1}-\Psi_{j-1}}{2h}\,, & \partial_X X\Psi&\to\frac{X_{j+1}\Psi_{j+1}-X_{j-1}\Psi_{j-1}}{2h}\,.\end{aligned}\tag{89}$$

For our understanding of stability, choose a point far from the resonance $X_j=jh$ and treat $X_{j\pm1}\approx X_j$ in what follows. Now consider the behaviour of plane waves,

$$\Psi_{j+1}=e^{iKh}\Psi_j\,,\tag{90}$$

through the discrete dynamical system given by substituting (89) into (87) and (88). This sort of analysis is called von Neumman stability analysis. In this case, the system is said to be stable at a given point X_j outside of the tunneling region if their are solutions for real K for any given real η^2. If the scheme is stable for all X_j outside the tunneling region, we call the scheme stable.

Under the plane wave assumption (90), through (89), we obtain a discrete operator-symbol

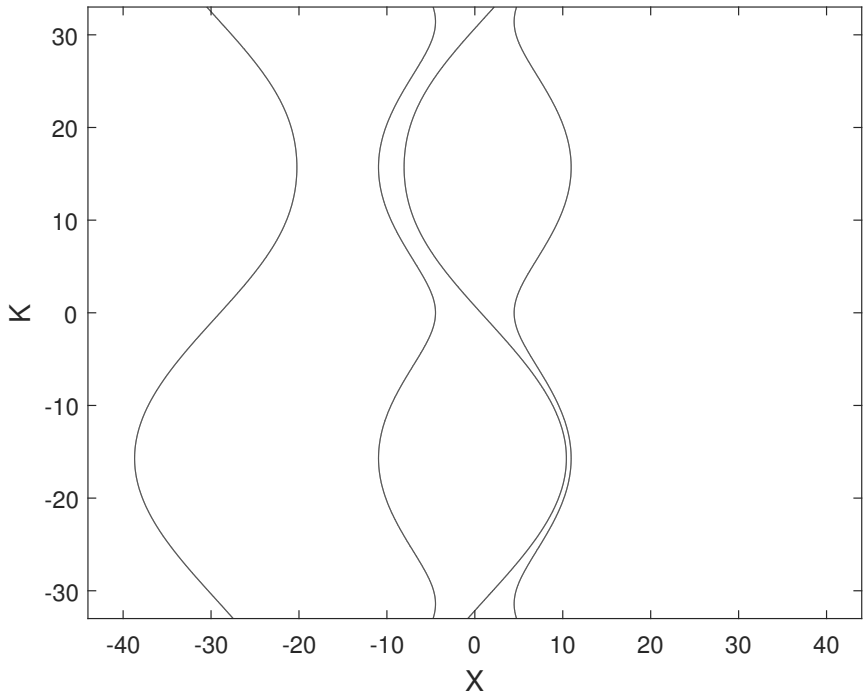

Figure 6. The discrete dispersion surface with $\omega = 1$, $\alpha = 0.1$, and $h = 0.1$.

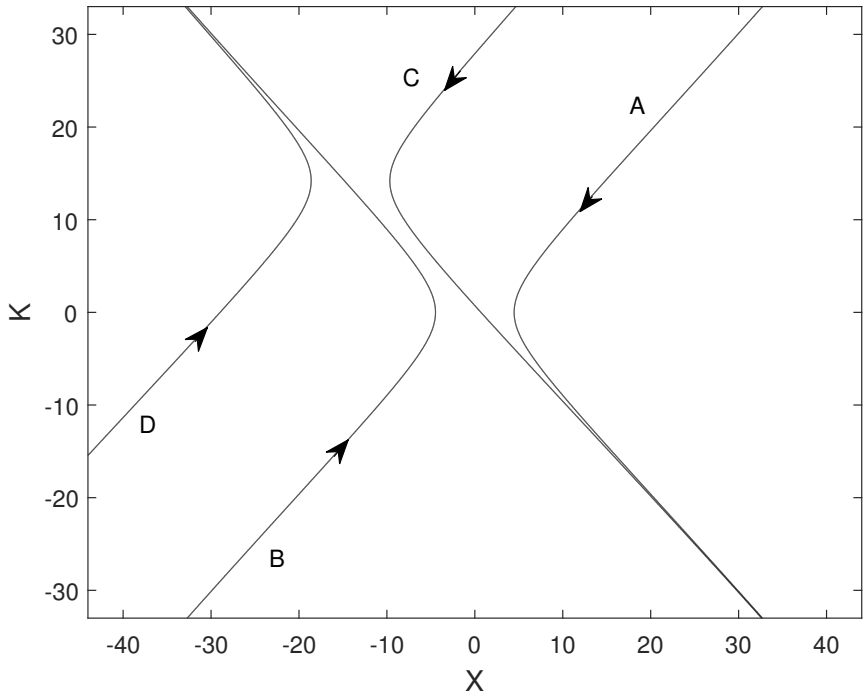

Figure 7. The discrete dispersion surface with $\omega = 1$, $\alpha = 0.1$, and $h = 0.01$.

relationship governed by our choice of discretization:

$$\begin{aligned} \partial_X &\to i\frac{\sin Kh}{h}\,, & \partial_X^2 &\to -\frac{\sin^2 Kh}{h^2}\,, \\ X\partial_X &\to iX\frac{\sin Kh}{h}\,, & \partial_X X &\to \frac{X_{j+1}e^{iKh} - X_{j-1}e^{-iKh}}{2h}\,. \end{aligned} \tag{91}$$

In the limit $h \to 0$, these return to the relationships predicted under the Weyl symbol calculus without the Moyal terms.

Similar to the eikonal analysis, we will assume that $\partial_X X\Psi \approx X\partial_X\Psi$. The discrete dispersion matrix is then given by

$$\begin{pmatrix} \frac{1}{2}\left(X^2 + 2X\frac{\sin Kh}{h} + \frac{\sin^2 Kh}{h^2}\right) & i\frac{\sin Kh}{\sqrt{2}h} + \frac{i}{\sqrt{2}}X - i\frac{\sin^2 Kh}{2h^2} + \frac{i}{2}X^2 - i\eta^2 + \frac{1}{2} \\ -i\frac{\sin Kh}{\sqrt{2}h} - \frac{i}{\sqrt{2}}X + i\frac{\sin^2 Kh}{2h^2} - \frac{i}{2}X^2 + i\eta^2 + \frac{1}{2} & 1 \end{pmatrix}. \tag{92}$$

The discrete dispersion surface is then the null space of this matrix. Examples of this surface are given in Figures 6 and 7.

Evidently, for sufficiently small h, we are able to recover the expected behaviour of the continuum dispersion relation. This implies that the scheme will be stable for sufficiently small h.

3c. Computation of the transmission coefficient

The numerical scheme is a second order scheme, so we need information about both Ψ and $\partial_x\Psi$ at some initial point X_0. We are interested in measuring how a mode within the event horizon tunnels outside of the event horizon. In terms of the rotated coordinates, we are interested in waves beginning on ray A of Figure 7 which then propagates to the left on the outgoing ray that smoothly connects to the ray labelled B. However, our equations have the temporal component Fourier transformed out, meaning that the incoming and the reflected waves are overlayed. Since we do not know the magnitude of the reflected component,

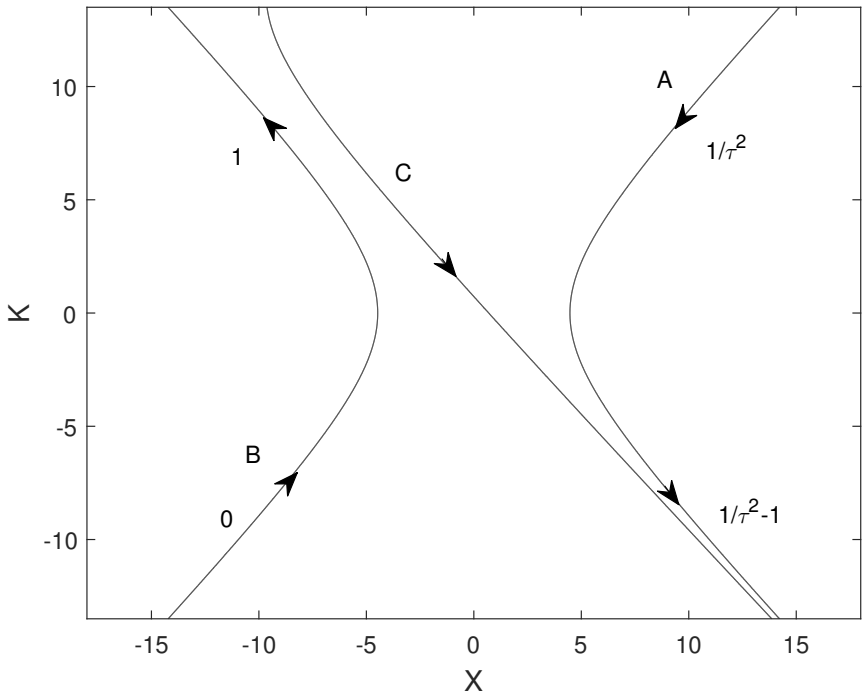

Figure 8. The surface $\det \mathsf{D}'(X,K) = 0$ for $\eta^2 = 4$. In our extraction of the transmission coefficient, we assume that there is no energy on the incoming mode labelled 0. Setting the action on the outgoing mode to one, we conclude that the incoming mode has action flux density $\mathscr{J} = 1/\tau^2$ and the reflected mode has action flux density $\mathscr{J} = 1/\tau^2$-1. In the calculation of the Hawking result, we assumed that the incoming mode of type 2 has no effect. The numerical simulations test this assumption.

this makes initialization inside the event horizon troublesome. However, to the left of the tunneling region, we only have an outgoing wave. That is to say, waves lies solely on the leftgoing component of ray B. Therefore, it makes sense to initialize on ray B and integrate our numerical scheme opposite to the direction of propagation. What we are then measuring is the incoming wave necessary to create our desired outgoing mode.

As the normal form analysis suggests that we are dealing with a scalar tunneling problem, we expect that as long as we initialize along a single branch – either the branch undergoing tunneling, or the "incoming" branch – of the dispersion relation all information will stay on that branch. Hence, the incoming and reflected wave will have wavenumbers of equal magnitude at each point X. Locally, this means that far from $X = 0$, the wavefunction has

the form

$$\Psi = \hat{\mathbf{e}} \left(A e^{-i\Theta(X)} + B e^{i\Theta(X)} \right) . \tag{93}$$

As discussed in our normal form analysis, the relevant polarization is

$$\hat{\mathbf{e}} = \hat{\mathbf{e}}_{-} \propto \begin{pmatrix} \sqrt{2} \\ i(X+K) \end{pmatrix} . \tag{94}$$

Measuring A will allow us to determine the tunneling coefficient. Setting the transmitted amplitude at $\Psi(-X_0) = 1$, we expect that

$$A = \frac{1}{\tau^2} , \quad B = A(1-\tau^2) = \frac{1-\tau^2}{\tau^2} \tag{95}$$

(see Figure 8) Hence, (93) at $X = X_0$ becomes becomes

$$\Psi(x_0) = \frac{1}{\tau^2} e^{-i\Theta(X_0)} + \frac{1-\tau^2}{\tau^2} e^{i\Theta(X_0)} . \tag{96}$$

Equivalently, we may write

$$\|\Psi\|^2 = \frac{1}{\tau^4} + \frac{1-\tau^4}{\tau^4} + 2\frac{1-\tau^2}{\tau^4} \cos\Theta . \tag{97}$$

From our discussions of ray tracing in Chapter 1, when the eikonal limit is valid (for large $|X|$), $\|\Psi\|^2 \propto v_g^{-1}$. Hence we are able to normalize the amplitude by the square root of the group velocity. Therefore, we can average $\|\Psi\|^2$ over a range of $[X_0, X_1]$:

$$\langle \|\psi\|^2 \rangle \equiv \frac{1}{h(|X_1 - X_0|)} \sum_j \|\Psi_j\|^2 . \tag{98}$$

If the average range is sufficiently large enough, we have that

$$\frac{1}{h(|X_1 - X_0|)} \sum_j \cos\Theta \approx 0_j . \tag{99}$$

Since $\langle \|\psi\|^2 \rangle$ is straightforward to compute numerically, we are left with the equation

$$\langle \|\psi\|^2 \rangle = \frac{2}{\tau^4} - 1 \,. \tag{100}$$

Multiplying through by τ^4, we are left with a simple polynomial equation which we can solve for τ.

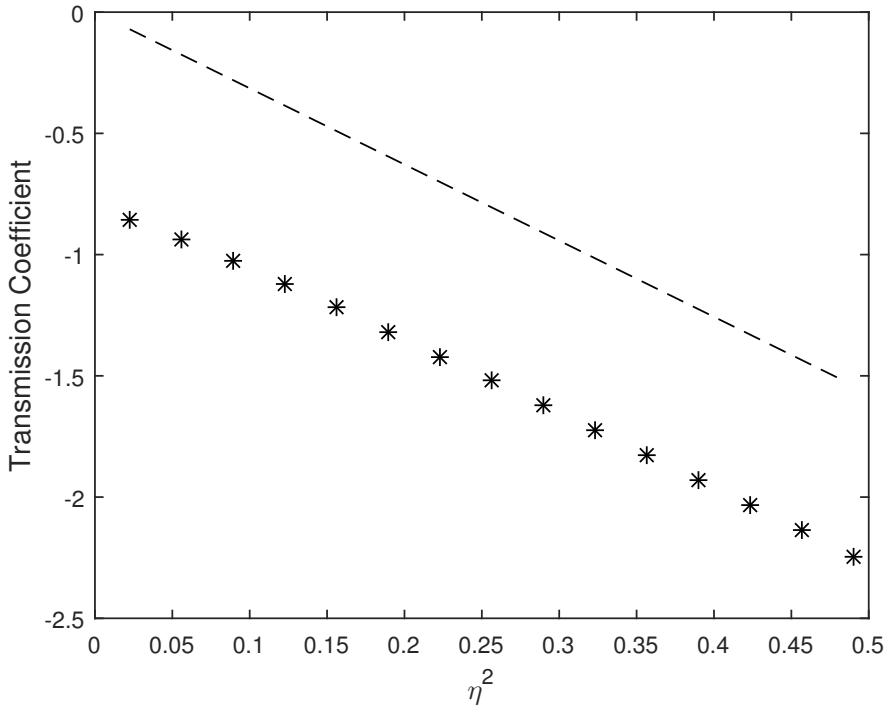

Figure 9. Calculated transmission coefficients over a range of η^2 values. The dotted line is the predicted value, calculated from (26). The points $*$ are the numerically computed tunneling coefficients.

The results are seen in Figure 9. Recall from Section 1 that we predict

$$\tau = e^{-\pi\eta^2} \,. \tag{101}$$

The results seen in Figure 9 instead suggest

$$\tau_{\text{numerical}} = e^{a-\pi\eta^2} = e^a e^{-\pi\eta^2} \,, \tag{102}$$

for some $a \in \mathbb{R}$. That is to say, the thermal spectrum of the event horizon is still present, but the power is scaled by some constant factor. The crux of the result is present – white noise on the event horizon of an acoustic black hole produces a thermal spectrum. The discrepancy between the theory and the measured result is likely a technical issue in the calculation, such as an issue in normalization. This issue will need to be resolved in future work.

4. Conclusions

We have thus demonstrated both numerically and through direct computation that acoustic Hawking radiation is a classical tunneling process. The discrepancies between the numerical and the theoretical work are not essential, though work remains to resolve the discrepancy. There are this a few directions in which we may proceed.

For instance, we may note that neither fluids nor black holes live in one dimension. In fact, even two dimensions in not quite sufficient – a proper analysis would require three. Though it may be possible to reduce these problems to a single dimension, such a reduction will definitely make approximations. Six dimensional ray phase space can lead to a more complicated phenomena that two dimensional ray phase space, such as focusing caustics. Furthermore, in higher dimensions the geometry of the even horizon may have significant effects. Therefore, an extension of the theory to higher dimensions would be a worthwhile, and likely nontrivial, pursuit.

Alternatively, we may move away from the black hole analogy and instead investigate the behavior of linear waves in varying flows. The ideal playground for this would be the linearized MHD equations, since they already have a self-adjoint formulation given in [9]. MHD allows for a variety of waves at different propagation speeds, and the effects of variations in background flow on different waves may lead to phenomena potentially of astrophysical interest.

THE END

Bibliography

[1] W. G. Unruh, "Experimental black-hole evaporation?," *Phys. Rev. Lett.*, vol. 46, pp. 1351–1353, May 1981.

[2] E. R. Tracy and D. Zhigunov, "Hawking radiation and classical tunneling: A ray phase space approach," *Physics of Plasmas*, vol. 23, no. 1, 2016.

[3] S. W. Hawking, "Particle creation by black holes," *Communications in Mathematical Physics*, vol. 43, no. 3, pp. 199–220, 1975.

[4] W. G. Unruh, "Notes on black-hole evaporation," *Phys. Rev. D*, vol. 14, pp. 870–892, Aug 1976.

[5] T. Jacobson, "On the origin of the outgoing black hole modes," *Phys. Rev. D*, vol. 53, pp. 7082–7088, Jun 1996.

[6] M. Visser, "Hawking radiation without black hole entropy," *Phys. Rev. Lett.*, vol. 80, pp. 3436–3439, Apr 1998.

[7] "Acoustic black holes: horizons, ergospheres and hawking radiation," *Classical and Quantum Gravity*, vol. 15, no. 6, p. 17671791, 1997.

[8] E. R. Tracy, A. J. Brizard, A. S. Richardson, and A. N. Kaufman, *Ray tracing and beyond: ray space methods in plasma wave theory.* Cambridge, 2014.

[9] A. J. Brizard, "Hermitian structure for linearized ideal mhd equations with equilibrium flows," *Physics Letters A*, vol. 168, no. 5, pp. 357 – 362, 1992.

[10] "*NIST Digital Library of Mathematical Functions.*" http://dlmf.nist.gov/, Release 1.0.14 of 2016-12-21. F. W. J. Olver, A. B. Olde Daalhuis, D. W. Lozier, B. I. Schneider, R. F. Boisvert, C. W. Clark, B. R. Miller and B. V. Saunders, eds.

[11] A. S. Richardson, E. R. Tracy, and A. N. Kaufman, "Higher order corrections to resonant mode conversion," *AIP Conference Proceedings*, vol. 933, no. 1, pp. 467–470, 2007.